International Journal of Bifurcation and Chaos, Vol. 10, No. 7 (2000) 1709–1728


# DYNAMICS OF THREE COUPLED EXCITABLE CELLS WITH $D_3$ SYMMETRY

M. SIGMAN* and B. G. MINDLIN†
*Facultad de Ciencias Exactas y Naturales,*
*Universidad de Buenos Aires, Pabelln I, Ciudad Universitaria,*
*(1428) Capital Federal, Argentina*

Received December 9, 1998; Revised December 3, 1999

We study the solutions of a system of three coupled excitable cells with $D_3$ symmetry. The system has two parameters, one controls the local dynamics of each cell and the other the strength of the coupling. We find and describe self-sustained collective oscillations. Periodic solutions appear in global bifurcations, typically after the collapse of fixed points heteroclinically connected. The symmetries of these periodic solutions are the same as the ones expected in periodic solutions which appear in local (Hopf) bifurcations.

## 1. Introduction

Many systems in nature present what is known as excitability. A system is said to be excitable whenever it presents a stationary solution towards which the system can evolve, after a perturbation, in two qualitatively different ways: either through a short trip in phase space, or through a large excursion in phase space, provided that the perturbation overcomes a given threshold. The canonical example of a natural system displaying excitable behavior is the neuron [Murray, 1989; Hodgin & Huxley, 1952], although many other systems are known to present this property. For example, recently it was proposed that a semiconductor laser with optical feedback presents excitable dynamics [Giudicci *et al.*, 1997].

In this work, we analyze the collective behavior of a small set of coupled excitable systems. For coupled oscillators, the theory of local bifurcations in the presence of symmetries allows us to classify with group theoretical tools the collective dynamical regimes that arise, in Hopf bifurcations, provided that the coupling is symmetric [Golubitsky, *et al.*, 1988]. In our case, we follow the spirit of these works in order to explain the collective features that arise when excitable systems are symmetrically coupled, typically after global bifurcations. We will show that self-sustained oscillations can arise, and that the existence of symmetric invariant subspaces of the phase space allows the system to undergo global bifurcations inheriting the symmetry of the subspaces. The symmetries of the periodic solutions are the same as the ones expected in Hopf (local) bifurcations, thus, we show that solutions that can be obtained using symmetry and Hopf bifurcation also appear in excitable systems.

The manuscript is organized as follows: in Sec. 2 we present our model, in Sec. 3 we build our coupled set. Section 4 contains the description and analysis of the solutions that we found, and we close with Sec. 5, containing our conclusions.

*Author for correspondence. E-mail: mariano@funes.rockefeller.edu
Current address: Center for Studies in Physics and Biology, The Rockefeller University, 1230 York Avenue, NY 10021, USA.
†E-mail: gabriel@birkhoff.df.uba.ar

## 2. Models for Excitability

### 2.1. *Excitability and Andronov bifurcation*

As mentioned in the introduction, a system is said to be excitable when it satisfies the following conditions [Murray, 1989]:

- It has a stable fixed point.
- Initial conditions over a given threshold return to the fixed point after a long (nonlocal) trip in phase space, while conditions below this threshold return to the fixed point in a short (local) trip.
- For initial conditions over the threshold, the response is stimulus independent.

In order to build a model presenting the dynamical features mentioned above one can request the existence of:

- a stable fixed point;
- an unstable fixed point (the threshold being a measure of the distance in phase space between the stable fixed point and the unstable one);
- an attractive connection between the saddle and the stable fixed point (a trajectory close to this connection will be the excited return trip).

If the global connection is highly attractive, the dynamics of the system collapses to a set with the topology of $S_1$, with two fixed points, one stable and one unstable, where the unstable manifold of the unstable fixed point feeds the stable fixed point. This scheme is shown in Fig. 1. In summary, the dynamical ingredients are (a) a local condition: the system is close to a saddle-node bifurcation, and (b) a global condition: the two branches of the unstable manifold of the saddle, feed the node.

This scenario is present in the parameter space neighborhood of the Andronov bifurcation [Andronov *et al.*, 1973], and the simplest ordinary differential equation displaying it is:

$$\dot{\theta} = \mu - \cos(\theta)\,, \quad \theta \in S_1\,. \tag{1}$$

The bifurcation diagram for the Andronov bifurcation is shown in Fig. 1. For $\mu = 1$, both fixed points collide in a nonhyperbolic fixed point, and a periodic orbit appears for $\mu > 1$.

Periodic orbits arising in an Andronov bifurcation have two characteristics that distinguish them

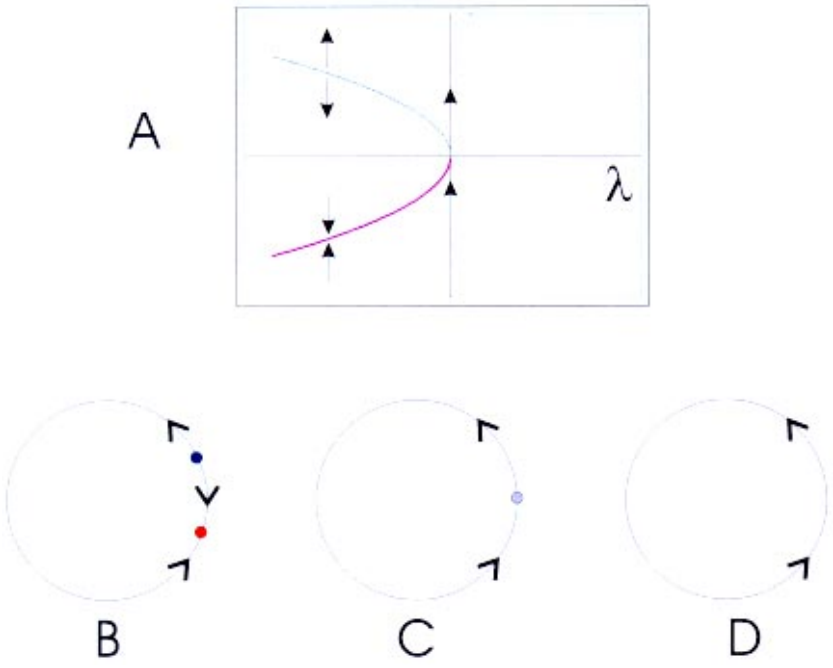


Fig. 1. (a) Bifurcation diagram for Andronov bifurcation, solid line corresponds to stable fixed point and dashed line to unstable. (b) Excitable system represented by Eq. (1) with $\mu < 1$. (c) Nonhyperbolic fixed point and homoclinic connection for $\mu = 1$ d. Periodic orbit for $\mu > 1$.

from periodic orbits arising in Hopf bifurcations, namely

- They appear with nonzero amplitude. That is:

$$\lim_{\lambda \to \lambda_0} A \neq 0 \tag{2}$$

  where $A$ is the amplitude, $\lambda$ the parameter and $\lambda_0$ the bifurcation point.
- They appear with infinite period. That is:

$$\lim_{\lambda \to \lambda_0} T = \infty \tag{3}$$

Even more, the orbit stays during a very long time (as long as we want if we are close enough to the bifurcation point) close to the point where the fixed points collapsed.

### 2.2. *Three symmetrically coupled cells*

The aim of this work is to study the dynamics of three excitable cells. We want these cells to be indistinguishable as well as the coupling between them. In Fig. 2 we represent each excitable system ("cell") by a circle, and the coupling by segments joining them. This coupling results in a system with $D_3$ or $S_3$ symmetry. ($S_3$ and $D_3$ are isomorphic groups that can be seen from the picture from the fact that the coupling of three cells to first neighbors is equivalent to coupling all with all. That is not true of course for more than three cells, just as for $n > 3$ $D_n$ is not isomorphic to $S_n$.)

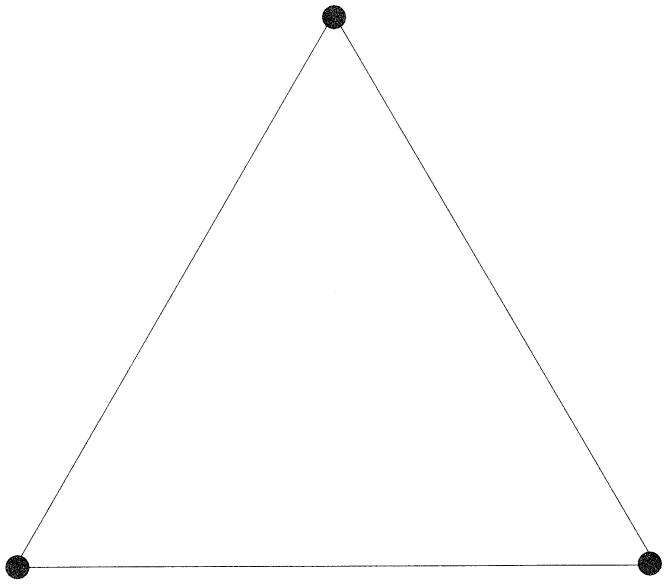

Fig. 2. Three coupled cells with $D_3$ symmetry.

Thus, our study will have two main ingredients: (a) excitability, a property of each of the cells we are coupling, and (b) symmetry, due to both the indistinguishibility of the three cells and the coupling between them.

It is known [Golubitsky *et al.*, 1988; Solari *et al.*, 1996] that symmetries impose a strong restriction in the generic solutions resulting from a bifurcation problem. The main idea is that when a solution with a given symmetry (which is described in terms of a subgroup $\Sigma$ of the total group of symmetry $\Gamma$) bifurcates, the bifurcating solutions generically lose not all, but some of its symmetries.

These ideas have been studied for the case of stationary and Hopf bifurcations with symmetry $D_n$ [Golubitsky *et al.*, 1988]. In the case of Hopf bifurcations, symmetry is not just broken in space coordinates, but in spatiotemporal coordinates, switching from a continuous symmetry ($t \to t + \delta t \ \forall t$, $\delta t$), corresponding to stationary solution, to a discrete symmetry ($t \to t + \mathcal{T} \ \forall t$, for a given $\mathcal{T}$). So when we look for the different symmetries of the solutions we will refer to spatial symmetries (invariance to operations in space) and spatiotemporal symmetries (invariance to only combined operation in space and time). We will summarize the known results for Hopf bifurcations in the presence of $D_3$ symmetry:

If a stationary solution $P(t) = (P_0, P_0, P_0)$, with maximum symmetry, bifurcates to a periodic orbit in a Hopf bifurcation then, generically the symmetry of the solution will be:

A. Spatial Symmetry:
   $x_i = x_j$. This corresponds to two oscillators in phase, and is invariant under the spatial operation

$$\begin{aligned} x_i &\to x_j \\ x_j &\to x_i \end{aligned} \tag{4}$$

   We will refer to solutions with this symmetry as solutions of Type B.
B. Spatiotemporal symmetry:
   $x_1(t) = x_2(t - (T/3)) = x_3(t - (T/3))$ where $T$ is the period of the solution. This corresponds to a rotating wave and is invariant under the operation:

$$\begin{aligned} x_1 &\to x_2 \\ x_2 &\to x_3 \\ x_3 &\to x_1 \\ t &\to t - \frac{T}{3} \end{aligned} \tag{5}$$

We will call this solution Rotating Wave or Type A solution.

$x_i(t) = x_j(t - (T/2))$, $x_k(t) = x_k(t - (T/2))$, where $T$ is the period of the solution. These solutions correspond to two oscillators half a period out of phase. The period of the third oscillator, in order to be invariant to the half period time translation, has to have period $T/2$. This solution is invariant under the operation:

$$\begin{aligned} x_i &\to x_j \\ x_j &\to x_i \\ x_k &\to x_k \\ t &\to t - \frac{T}{2} \end{aligned} \tag{6}$$

## 3. Three Coupled Excitable Cells

### 3.1. *Building the system*

We saw in the introduction that the system:

$$\dot{\theta} = \mu - \cos(\theta) \tag{7}$$

where $\theta \in S_1$ and $\mu < 1$, was the simplest system that included the two main ingredients to obtain excitable behavior, provided that the system was close to a saddle-node bifurcation.

We want to see what happens when we couple three of these excitable cells. To establish the coupling we extend the system described by Eq. (7) to a two-dimensional system with an invariant circle with the condition that the dynamics restricted to this invariant circle is given by Eq. (7). We do that in order to define the coupling in terms of the Cartesian variables.

The system:

$$\begin{aligned} \dot{x} &= -y(\mu - x) + x(1 - (x^2 + y^2)) \\ \dot{y} &= x(\mu - x) + y(1 - (x^2 + y^2)) \end{aligned} \tag{8}$$

after the transformation:

$$\begin{aligned} r\dot{r} &= x\dot{x} + y\dot{y} \\ \dot{y}x - \dot{x}y &= r^2\dot{\theta} \end{aligned} \tag{9}$$

is, written in polar coordinates:

$$\begin{aligned} \dot{r} &= r(1 - r^2) \\ \dot{\theta} &= \mu - \cos(\theta) \end{aligned} \tag{10}$$

so that the system described by Eqs. (8) is the planar system that satisfies: (a) the dynamics restricted to the circle of radius 1 is the one given by Eq. (7) and (b) this circle is an attracting set.

We now write the coupling adding the constraint that the three tori stays as an invariant set in the presence of the coupling, so we can study the dynamics of the system through the angular variables alone. That is, $\dot{r}_i|_{(r_i=1)} = 0$, $i = 1, 2, 3$.

Moreover, we want the coupling to satisfy the following conditions:

- **Symmetry**: The symmetry of the system in the presence of the coupling, remains $D3$.
- **Linearity**: The coupling is linear in the Cartesian coordinates.
- **Relative differences**: The coupling is proportional to the relative differences between each of the cells. In particular two cells are uncoupled when they are in the same state.

The general expression for a coupling satisfying these three conditions is [Golubitsky *et al.*, 1988]:

$$\begin{aligned} \frac{d(x_i, y_i)}{dt} &= F(x_i, y_i, \mu) + K(\varepsilon, \lambda) \\ &\quad \cdot (2x_i - x_j - x_k, 2y_i - y_j - y_k) \end{aligned} \tag{11}$$

where $F(x_i, y_i)$ represents the local dynamics of each cell and the second term to the coupling satisfying the last three conditions.

We choose as a coupling matrix:

$$\mathbf{K}(\varepsilon) = \begin{pmatrix} -\varepsilon & 0 \\ 0 & \varepsilon \end{pmatrix}$$

As an example, for cell number 1, Eq. (11) can be written as:

$$\begin{aligned} \frac{dx_1}{dt} &= f(x_1, y_1, \mu) - \varepsilon(x_1 - x_2) - \varepsilon(x_1 - x_3) \\ \frac{dy_1}{dt} &= g(x_1, y_1, \mu) + \varepsilon(y_1 - y_2) + \varepsilon(y_1 - y_3) \end{aligned} \tag{12}$$

after this, the physical meaning of the coefficients of the matrix $K(\varepsilon)$ becomes clear. They give a measure of the strength of the coupling. If the coefficient is negative (as is the case for the coupling of the $\hat{x}$ coordinates), the coupling is restitutive. If the coefficient is positive this will work increasing the difference between the values of the dynamical variables of the different cells.

We now rewrite the coupling in terms of the angular variables, using the constraint $\dot{r}_1|_{(r_1=1)} = \dot{r}_2|_{(r_2=1)} = \dot{r}_3|_{(r_3=1)} = 0$ and obtain the equation

for the phases:

$$\begin{aligned}\dot{\theta}_1 &= \mu - \cos(\theta_1) + 2\varepsilon \cdot (2\,\sin(2\cdot\theta_1) \\ &\quad - \sin(\theta_1+\theta_2) - \sin(\theta_1+\theta_3)) \\ \dot{\theta}_2 &= \mu - \cos(\theta_2) + 2\varepsilon \cdot (2\,\sin(2\cdot\theta_2) \\ &\quad - \sin(\theta_2+\theta_1) - \sin(\theta_2+\theta_3)) \\ \dot{\theta}_3 &= \mu - \cos(\theta_3) + 2\varepsilon \cdot (2\,\sin(2\cdot\theta_3) \\ &\quad - \sin(\theta_3+\theta_1)\sin(\theta_3+\theta_2))\end{aligned} \tag{13}$$

We will study the system and its different solutions in parameter space. Before searching for the different solutions we want to make the following remarks.

- **Invariant Manifolds.** The manifold $\theta_1 = \theta_2 = \theta_3$ is a one-dimensional manifold with the topology of $S_1$. The invariance of the manifold implies that if a given point $\hat{p}$ belongs to the manifold, its orbit will also belong to the manifold, or in other words, if the three cells are originally in phase they will be for ever in phase.

  The three manifolds $\theta_i = \theta_j$ with $(i,\, j) = (1,\, 2)$, $(1, 3)$ or $(2, 3)$, are invariant two-tori. Each of them corresponds to two cells in phase. The intersection of these three manifolds is one-dimensional, $\theta_1 = \theta_2 = \theta_3$.

  By equivariance, anything that happens in one of the two-tori, happens in the other two.
- **Excitability and individual behavior of each cell.** Each individual cell (uncoupled from the others), for $\mu < 1$, has an excitable behavior, which implies it does not oscillate. For $\mu > 1$ a periodic orbit appears in an Andronov bifurcation. The two main characteristics of this periodic solution are that it appears with infinite period and nonzero amplitude. It is important to remember the properties of one cell, to understand the emerging properties of the system.
- **Coordinate System.** We will use two different representations to study the problem. The first one corresponds to the identification of each angular variable with one Cartesian axis. The second representation, has the advantage that symmetry operations are more easily visualized, and has the disadvantage that the quotients are harder to visualize. We define those coordinates in the following way [Ashwin *et al.*, 1990]. A real variable $\Theta$ which corresponds to the average phase, that is: $\Theta = (\theta_1 + \theta_2 + \theta_3)/3$, and a complex variable $\phi = \theta_1 + e^{\frac{i2\pi}{3}}\theta_2 + e^{\frac{i4\pi}{3}}\theta_3$. The invariant manifolds in this coordinate system are shown in Table 1. The action of the symmetry group corresponds to (Fig. 3):
  — Rotation of $2\pi/3$ around the $\Theta$ axis, the cycle (312).
  — Complex conjugation ($\phi \to \overline{\phi}$) the permutation (23).

  The axis $\hat{\Theta}$ corresponds to the diagonal of the cube given by the direction $(1, 1, 1)$ and is invariant under all the symmetry operations of D3 (Fig. 3).

## 4. Results

### 4.1. *Three quiescent cells*

Let us first analyze the fixed points of our system. Each individual cell has two fixed points:

- $\theta = -\arccos(\mu) \to$ (stable)
- $\theta = \arccos(\mu) \to$ (unstable)

Table 1. Invariant manifolds in the symmetric representation.

| Manifold | Coordinates | Dimension |
|---|---|---|
| $\theta_1 = \theta_2$ | $\mathrm{Arg}(\phi) = e^{\frac{i4\pi}{3}}$ | 2 |
| $\theta_1 = \theta_3$ | $\mathrm{Arg}(\phi) = e^{\frac{i2\pi}{3}}$ | 2 |
| $\theta_2 = \theta_3$ | $\mathrm{Im}(\phi) = 0$ | 2 |
| $\theta_1 = \theta_2 = \theta_3$ | $\phi = 0$ | 1 |

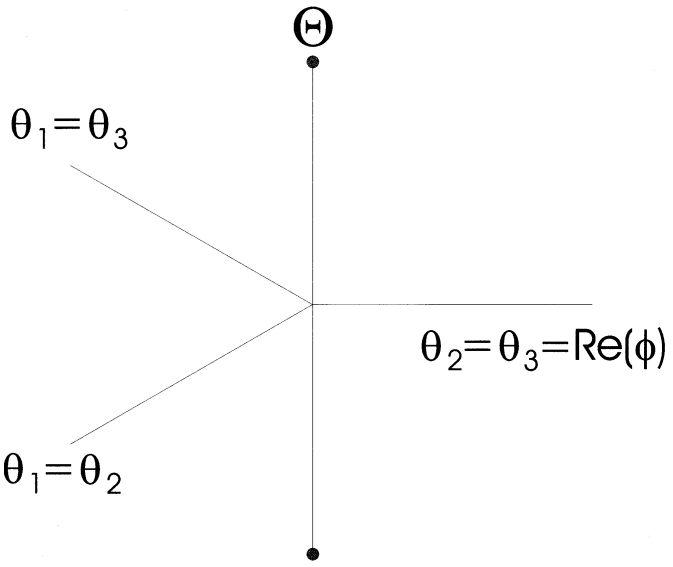


Fig. 3. Invariant circle $\theta_1 = \theta_2 = \theta_3$ corresponds to the $\Theta$ axis in the symmetric representation. Points marked with dots are identified by the quotient.

Therefore, $\theta_1 = \theta_2 = \theta_3 = -\arccos(\mu)$ and $\theta_1 = \theta_2 = \theta_3 = \arccos(\mu)$ are fixed points for the system of three coupled cells.

We will call these points $P1$ and $P2$ respectively. From now on, we will identify numbers with different fixed points that will appear in parameter space. The fixed point $P2$ will always be unstable which can be seen from the fact that the eigenvalue in the $(1,1,1)$ direction is $\sqrt{1-\mu^2}$ which is positive. We want to study the stability of $P1$. In order to do that we compute $Df(P1, \varepsilon, \mu)$, where $f$ is the vector field describing the three coupled cells [Eqs. (13)]. The diagonal form of $Df(P1, \varepsilon, \mu)$ is:

$$\mathbf{Df(P1)} = \begin{pmatrix} -\sqrt{1-\mu^2} & 0 & 0 \\ 0 & 3\varepsilon(2\mu^2-1) - \sqrt{1-\mu^2} & 0 \\ 0 & 0 & 3\varepsilon(2\mu^2-1) - \sqrt{1-\mu^2} \end{pmatrix}$$

where the first eigenvalue is associated with the $(1,1,1)$ direction, and the remaining two, to the degenerated orthogonal plane.

We can see that the eigenvalue associated to the $(1,1,1)$ direction does not depend on $\varepsilon$, which we could expect since in this subspace, the cells are in phase and therefore they are uncoupled. In the same way we do not need any computation to realize that this direction is always stable, as each cell has a stable fixed point in $\theta = -\arccos(\mu)$, and the restriction of the dynamics to this subspace is just the overlap of the local dynamics for each of the oscillators. When restricted to the $(1,1,1)$ direction, there are three identical and uncoupled oscillators.

The remaining eigenvalues change sign (therefore the fixed point loses stability in the plane normal to $(1,1,1)$) when:

$$\varepsilon = \frac{\sqrt{1-\mu^2}}{3(2\mu^2-1)} \tag{14}$$

We see, as verified in the numerical analysis, that for $\varepsilon > 0$, when $\varepsilon$ is small, the fixed point is stable. In the case of $\mu > (1/\sqrt{2})$, for $\varepsilon$ large enough, it loses stability. Why do we need the condition $\mu > (1/\sqrt{2})$ for the system to lose stability? In order to explain this issue we have to come back to the idea of a two-dimensional system relaxing on $S_1$, and the relations [Fig. 4(a)]:

$$\delta x = -\sin(\theta)\delta\theta \quad \delta y = \cos(\theta)\delta\theta \tag{15}$$

If we perturb the system close to $\theta = -(\pi/2)$, and we force it to remain in the circle, we will have perturbed it almost in the direction $\hat{x}$, and in case we perturb it close to $\theta = 0$ with the same constraint, we will have perturbed it almost in the $\hat{y}$ direction.

Considering that the fixed point corresponds to $\theta = -\arccos(\mu)$, we can see that $\mu > (1/\sqrt{2})$ corresponds to $|\theta| < (\pi/2)$ and then, by what we just saw, we will be studying stability in the $\hat{y}$ direction.

The degenerated eigenvalues of $Df(P1, \varepsilon, \mu)$ can be split into two different terms:

$$\begin{aligned} -\sqrt{1-\mu^2} &\rightarrow \text{Local Dynamics} \\ 3\varepsilon(2\mu^2-1) &\rightarrow \text{Coupling} \end{aligned} \tag{16}$$

The couple matrix we chose was:

$$\mathbf{K}(\varepsilon) = \begin{pmatrix} -\varepsilon & 0 \\ 0 & \varepsilon \end{pmatrix}$$

That is, the coupling was stable (restitutive) in the "$\hat{x}$" direction and unstable in the "$\hat{y}$" direction. Then, as we can see in Fig. 4, when $\mu > (1/\sqrt{2})$ the

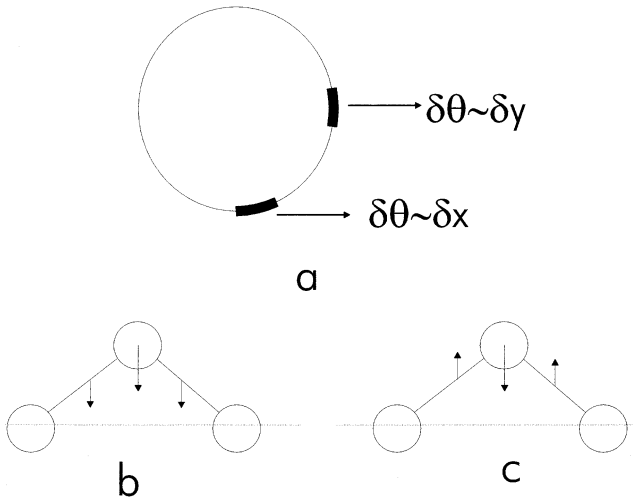


Fig. 4. (a) Geometric relation between $\delta\theta$, $\delta x$ and $\delta y$. (b) If $\mu < (1/\sqrt{2})$ both local dynamics of each cell and the coupling between them contribute to re-establishing a cell to its equilibrium position. (c) If $\mu > (1/\sqrt{2})$ there is a competition between local dynamics and the coupling.

stable local dynamics competes with the coupling, which destabilizes the system. For $\varepsilon$ large enough, that is, when coupling is strong enough to be the most important term, the fixed point loses stability. If $\mu < (1/\sqrt{2})$ there is no mechanism contributing to destabilize the fixed point and then, it is always stable.

Let us now study in more detail how this fixed point will lose stability. In order to do that we compute the center manifold (of a vector field depending on one parameter) and the dynamics restricted to the intersection of the center manifold at a neighborhood of the fixed point.

We have to write our vector field splitting it in two groups of coordinates whose tangent spaces correspond respectively to the center and stable manifolds of the linearized vector field [Wiggins, 1990]. That is we have to rewrite it in the following way:

$$\begin{aligned} \dot{x} &= Ax + f(x, y, \lambda) \\ \dot{\lambda} &= 0 \\ \dot{y} &= By + g(x, y, \lambda) \end{aligned} \tag{17}$$

where $A$ has all pure imaginary eigenvalues, and the eigenvalues of $B$ have all negative real components. Notice that $\lambda$ is a rescaling of the control parameter so that the bifurcation point corresponds to $\lambda = 0$.

When we split our vector field at the bifurcation point:

$$\varepsilon = \frac{\sqrt{1-\mu^2}}{3(2\mu^2-1)} \tag{18}$$

in directions which are tangent to the stable manifold $(1, 1, 1)$ and to the center manifold (orthogonal plane) we naturally find the symmetrical coordinates $(\Theta, \phi)$ that we defined before.

The fixed point $P1$ corresponds to $(\Theta = -\arccos(\mu),\ \phi = 0)$. The stable manifold is the $\hat{\Theta}$ axis and the plane $\Theta = -\arccos(\mu)$ is tangent to the center manifold. That is, the center manifold will locally be the graph of a function: $\Theta = h(\phi, \lambda(\varepsilon, \mu))$.

We want to find the first nonzero terms in a Taylor series for this function. Doing so with the $(\Theta, \phi)$ coordinates:

$$\begin{aligned} \dot{\Theta} = &-\sqrt{1-\mu^2}\Theta + \frac{1}{2}\mu\Theta^2 \\ &+ \left(\frac{\mu}{9} + \frac{2}{3}(a(\mu) + b(\mu)\lambda)\right)(v^2 + w^2) \end{aligned} \tag{19}$$

$$\begin{aligned} \dot{v} = &\lambda v + \left(\frac{\mu}{6} + \frac{3}{2}(a(\mu) + b(\mu)\lambda)\right)(v^2 - w^2) \\ &+ (\mu + 6(a(\mu) + b(\mu)\lambda))\Theta \cdot v \\ \dot{w} = &\lambda w + (\mu + 6(a(\mu) + b(\mu)\lambda))\Theta \cdot w \\ &- \left(\frac{\mu}{3} + 3(a(\mu) + b(\mu)\lambda)\right) vw \end{aligned}$$

$$a(\mu) = \frac{2\mu(1-\mu^2)}{3(2\mu^2-1)} \quad b(\mu) = \frac{2\mu\sqrt{1-\mu^2}}{3(2\mu^2-1)} \tag{20}$$

where $v = \mathrm{Re}(\phi)$, $w = \mathrm{Im}(\phi)$ and $\lambda = 3(2\mu^2 - 1)(\varepsilon - (-\sqrt{1-\mu^2}/3(2\mu^2-1)))$ is a rescaling of the parameter so the bifurcation point corresponds to $\lambda = 0$.

We want to remark that the terms $\lambda v$ and $\lambda w$ are nonlinear in the $(\Theta, v, w, \lambda)$ variables.

We propose a second-order polynomic expression for $h(v, w, \lambda)$

$$\begin{aligned} h(v, w, \lambda) = &a_1 v^2 + a_2 w^2 + a_3 \lambda^2 \\ &+ a_4 vw + a_4 \lambda v + a_6 \lambda w \end{aligned} \tag{21}$$

and solve the quasilinear partial derivative equation for which $h(v, w, \lambda)$ has to be a solution.

$$\begin{aligned} &\nabla h(v, w, \lambda) \cdot [(3\varepsilon(2\mu^2-1) - \sqrt{1-\mu^2})(v, w) \\ &\quad + f(h(v, w\lambda), v, w, \lambda)]\sqrt{1-\mu^2} \cdot h(v, w, \lambda) \\ &\quad - g(h(v, w, \lambda), v, w, \lambda) = 0 \end{aligned} \tag{22}$$

If we want second-order terms to be the same on both sides, we have:

$$a_1 = a_2 = \frac{\dfrac{\mu}{9} + \dfrac{2}{3}a(\mu)}{\sqrt{1-\mu^2}} = c(\mu)\,. \tag{23}$$

So the center manifold turns out to be locally a parabola whose slope does not depend on the parameter $\lambda$.

Let us now compute the dynamics restricted to the center manifold.

$$\begin{aligned} \dot{v} = &\lambda v + \left(\frac{\mu}{6} + \frac{2}{3}(a(\mu) + \lambda b(\mu))(v^2 - w^2)\right. \\ &\left. + O(\|(\lambda, v, w)\|^3)\right) \\ \dot{w} = &\lambda w - 2\left(\frac{\mu}{6} + \frac{2}{3}(a(\mu) + \lambda b(\mu))vw\right. \\ &\left. + O(\|(\lambda, v, w)\|^3)\right) \end{aligned} \tag{24}$$

or in its complex form:

$$\dot{\phi} = \lambda \cdot \phi + \left( \frac{\mu}{6} + \frac{2}{3}(a(\mu) + \lambda b(\mu))\hat{\phi}^2 \right). \qquad (25)$$

The dynamics in the intersection of the center manifold and the invariant two-tori ($\theta_2 = \theta_3$), which, as we saw before corresponds to $w = 0$ is,

$$\dot{v} = \lambda v + \left( \frac{\mu}{6} + \frac{2}{3}(a(\mu) + \lambda b(\mu))v^2 \right). \qquad (26)$$

The stationary solutions are the two fixed points:

$$\begin{aligned} v &= 0 \\ v &= \frac{-\lambda}{\left( \frac{\mu}{6} + \frac{2}{3}(a(\mu) + \lambda b(\mu)) \right)} \end{aligned} \qquad (27)$$

When $\lambda < 0$ the fixed point $v = 0$ is stable while the other is unstable.

When $\lambda = 0$ the unstable fixed point crosses the origin, changing stability, so that when $\lambda > 0$, $v = 0$ is unstable and the other is stable as we can see in Fig. 5. This bifurcation is known as transcritical.

In the other two intersections of the center manifold with an invariant manifold $\theta_1 = \theta_2$ ($w = \sqrt{3}v$) and $\theta_1 = \theta_3$ ($w = -\sqrt{3}v$) a transcritical bifurcation occurs, that is a fixed point crossing the origin and changing the stability with it. Solving Eq. (24) we can see that those four fixed points (the origin and the three crossing in each invariant two-tori) are all the solutions in a neighborhood of the origin.

Summarizing, $P1$ loses stability at $\lambda = 0$ in a degenerate way in the plane normal to the (1,1,1)

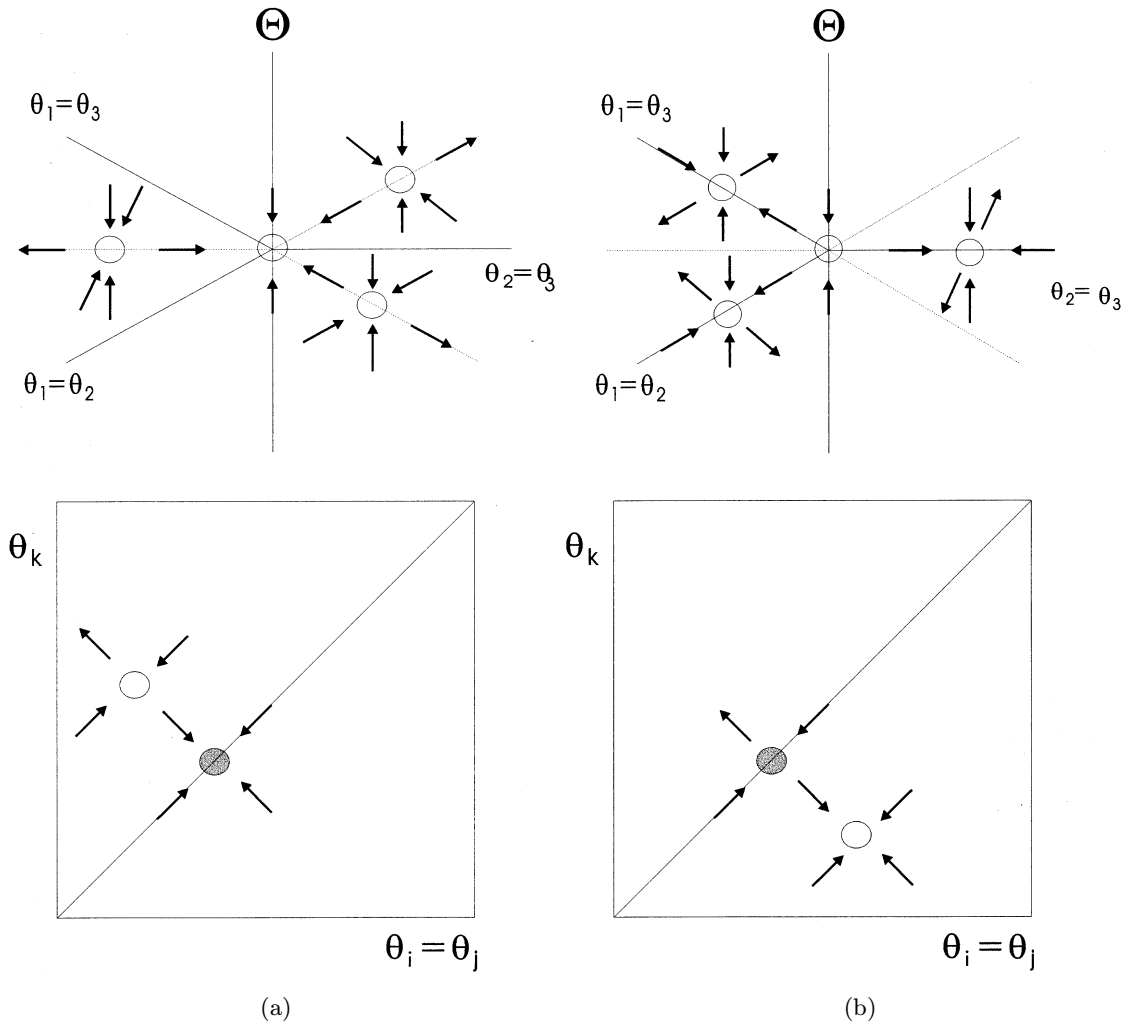


Fig. 5. Triple transcritical bifurcation. (a) Symmetric representation. (b) Representation in one of the invariant two-tori in Cartesian coordinates.

direction, and the three fixed points crossing simultaneously the origin in each invariant two-tori, in a triple transcritical bifurcation, gain the stability that the origin is losing. This is represented in Fig. 5. We will refer to the fixed points that cross the origin in the triple transcritical as $P3_1$, $P3_2$ and $P3_3$, or simply $P3$ to refer to a representative in one of the invariant two-tori.

### 4.2. *Bifurcation diagram*

In Fig. 6 we display the bifurcation diagram in the half-plane $\varepsilon$, $\mu$, ($\varepsilon > 0$). In Region I of the parameter space, the only stable solution is $P1$.

In each plane we have three unstable fixed points: $P2$, $P3$ and $P4$ as shown in Fig. 7. The fixed point $P2$, which we computed before, corresponds to $\theta_1 = \theta_2 = \theta_3 = \arccos(\mu)$. The fixed point $P3$, which we now find numerically, is the one that will later on cross the origin in the triple transcritical that we described before. The rest of the fixed points to which we will be referring to are found numerically.

When we cross the curve $\psi$ for example for $\mu = 0.8$ and go towards the Region II of the parameter space, two fixed points appear in each invariant two-tori $\theta i = \theta j$, a node and a saddle which we respectively call $P5$ and $P6$ (Fig. 8).

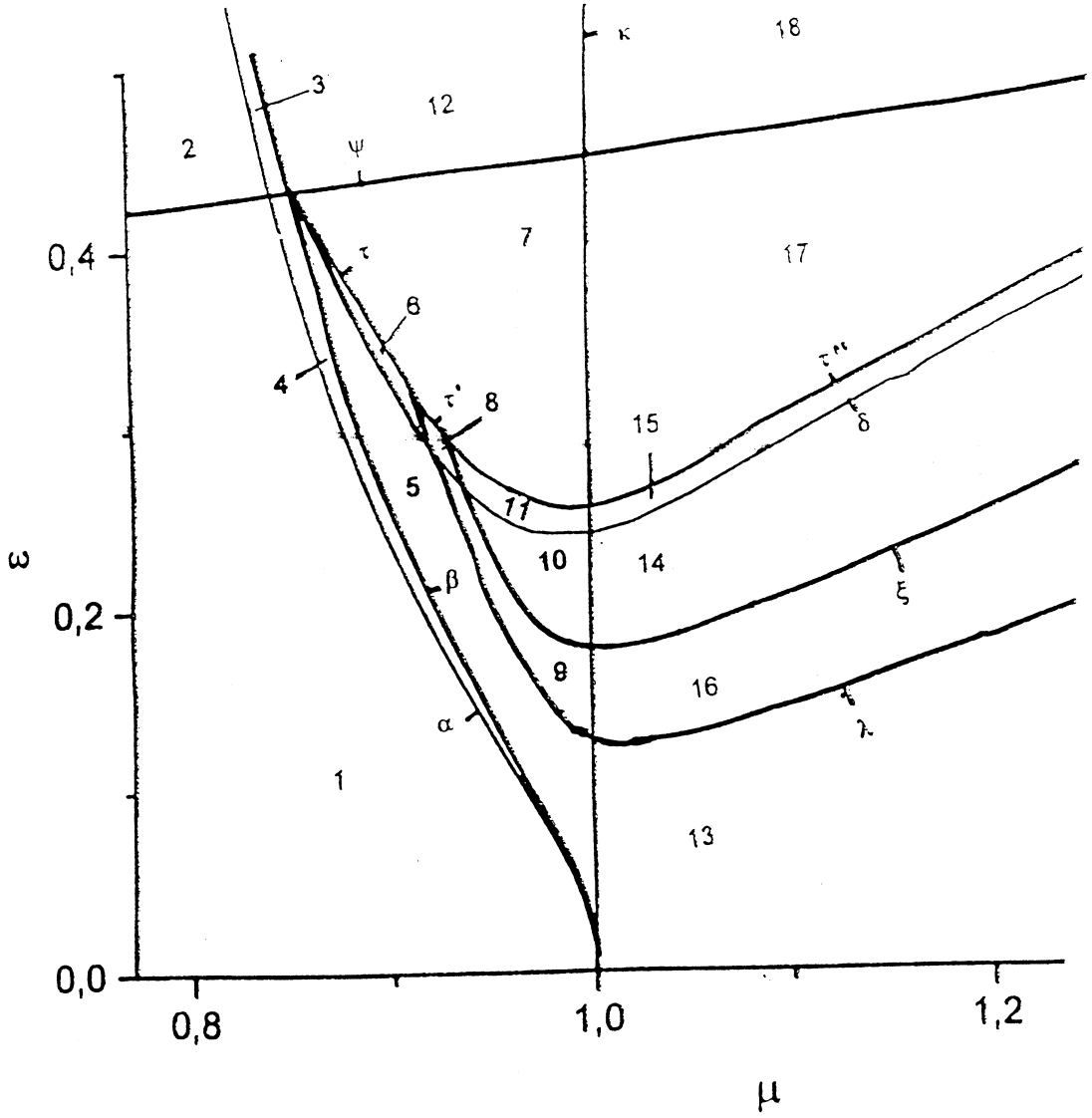


Fig. 6. Bifurcation diagram in the plane ($\varepsilon$, $\mu$).

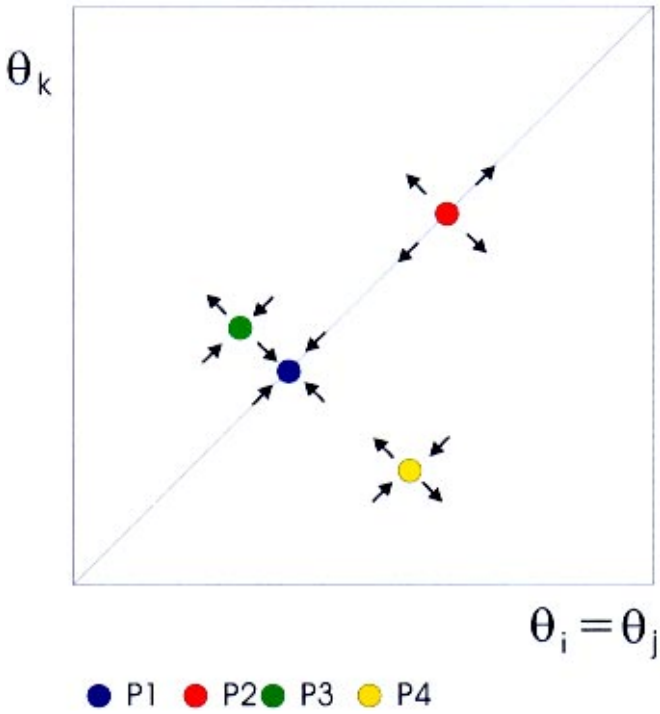


Fig. 7. Fixed Points in Region I. Representation in one of the invariant two-tori.

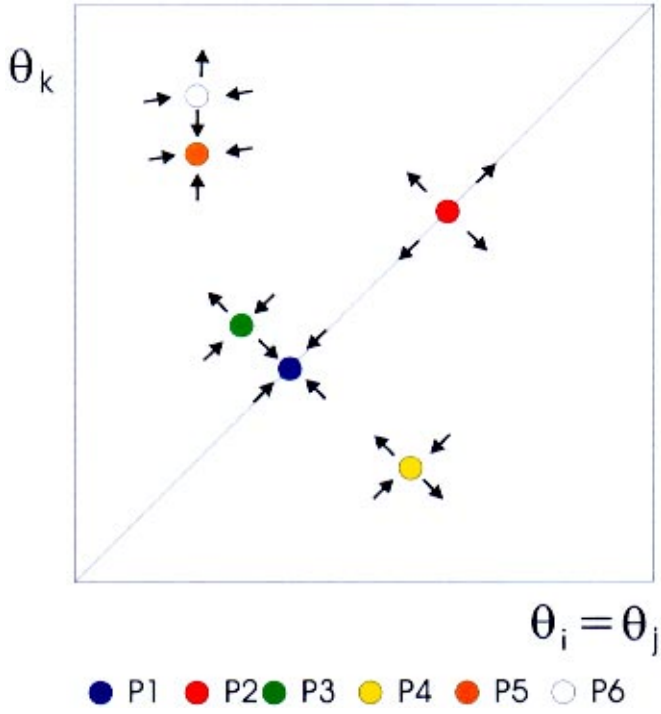


Fig. 8. Fixed Points in Region II. Representation in one of the invariant two-tori.

Thus the $\psi$ curve indicates a saddle-node bifurcation, in which the fixed points $P5$ and $P6$ are born. Those fixed points appear in a region in which the invariant two-tori locally attracts, so the node will not just be an attractor when restricted to the invariant manifold but will be an attractor when seen in $S_3$.

The $\alpha$ curve corresponds to the local triple transcritical bifurcation which we described above, in which $P3_1$, $P3_2$ and $P3_3$ cross the origin and $P1$ loses stability (Fig. 5).

When we cross the $\alpha$ curve from Region II to Region III, we have, as we saw, six fixed points in each invariant two-tori, $\theta i = \theta j$. We are interested in the following connection between stable and unstable manifolds of different fixed points. The fixed point $P6$ (a saddle), is feeding $P3$, which is an attractor when restricted to the two-tori. The unstable manifold of $P3$, which is locally normal to the invariant two-tori, feeds the conjugate of $P5$, that is, the equivalent to it in one of the other invariant two-tori. This is repeated in the three tori so that fixed points are connected as seen in Fig. 9.

Now we want to fix $\mu$ and go to the lower $\varepsilon$ to find the curve $\psi$. The fixed points $P5$ and $P6$ come together as we get closer to the $\psi$ curve. When we are just on it, they will have collapsed in a unique nonhyperbolic fixed point that we call $P$.

This nonhyperbolic fixed point $P$ is feeding $P3$ in its generalized (nonlinear) invariant manifold, as the saddle that just collapsed with $P$ did, and at the same time is being fed by the conjugated of $P3$ in the other invariant manifold, as happened with the node that just collapsed in $P$.

We then have the following connections which are shown in Fig. 10. The fixed point $P_1$ in the first two-tori (I) feeds $P3_1$ in the same two-tori (I). This one, through its invariant manifold feeds point $P_2$ in the second two-tori (II), which is connected with $P3_2$ in two-tori (II). Again the unstable manifold of this last fixed point is the stable manifold of $P_3$ in the third two-tori (III) which feeds $P3_3$ in the (III) two-tori, which finally, and closing the loop, is feeding the fixed point $P_1$ of the first (I) two-tori.

We then have a heteroclinic connection divided into six pieces, three living in the invariant tori and the other three jumping from one to the other. There is also a (conjugate) connection which goes through the invariant two torus counterclockwise, that is $(\mathrm{I}, \mathrm{III}, \mathrm{II})$.

This heteroclinic connection is not structurally stable, that is it does not live in an open set of

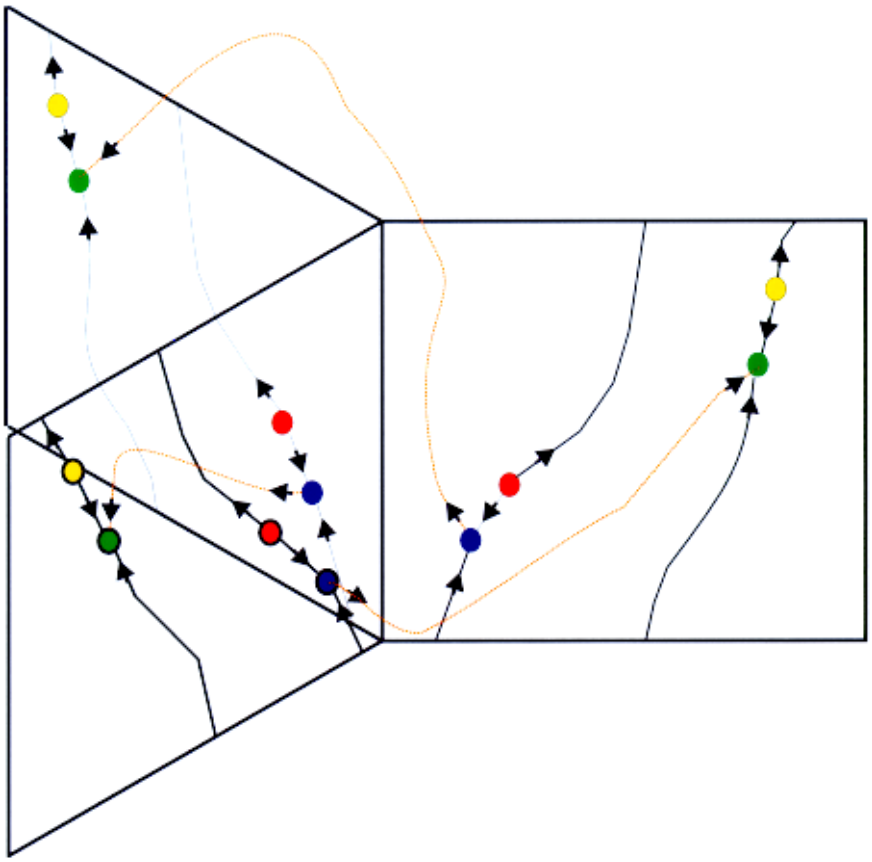

Fig. 9. One-dimensional manifolds of the fixed points before the heteroclinic connection (Region III).

parameter space. Over the $\psi$ curve it breaks because $P$ splits into two fixed points, and below it, because $P$ disappears. We want to know how the dynamics will be in Region IV of the parameter space, that is, what remains after the heteroclinic connection is broken due to the disappearance of $P$.

Let us follow the trajectory of an initial condition close to $P3$ of any of the invariant two-tori. The trajectory will go to look for the point $P$ in the next invariant tori, but it will no longer be there, so we will go on until $P3$ of this tori (to which we are close, but obviously never due to its invariance). When close to $P3$ we will be expelled in a similar trip to an inexistent $P$. This process is repeated three times until we arrive at a point close to where we started. That is, we expect a recurrence as a consequence of the broken heteroclinic cycle. We numerically observe that we not only have this recurrence (a well defined return map in an appropriate neighborhood of $P3$), but we find a periodic orbit (fixed point in this return map).

This dynamics can be studied by building a Poincaré Map as the composition of a local map and a global map that can be approximated by an affine map [Zimmerman & Natiello,1998; Wiggins, 1990]. The global map depends on some parameter and solutions that exist in open sets of this parameter space. This method can be used to prove the existence of periodic orbits for the generic case in which a heteroclinic connection, like the one we described, is broken.

At this point we want to make a remark related to the symmetry of this periodic solution. From our discussion, we not only saw that there was a recurrence, but that the orbit of a point $\overline{q}$ before returning (recurrence) close to $\overline{q}$ visited its conjugates.

Let us assume as an hypothesis that a point $\overline{q} = (q_1, q_2, q_3)$ evolves after a time $\tau$ to its conjugate $\overline{q}' = \gamma \cdot \overline{q} = (q_3, q_1, q_2)$, hypothesis that we verify numerically and could be checked with similar techniques to the ones we just mentioned to prove the existence of the periodic orbit.

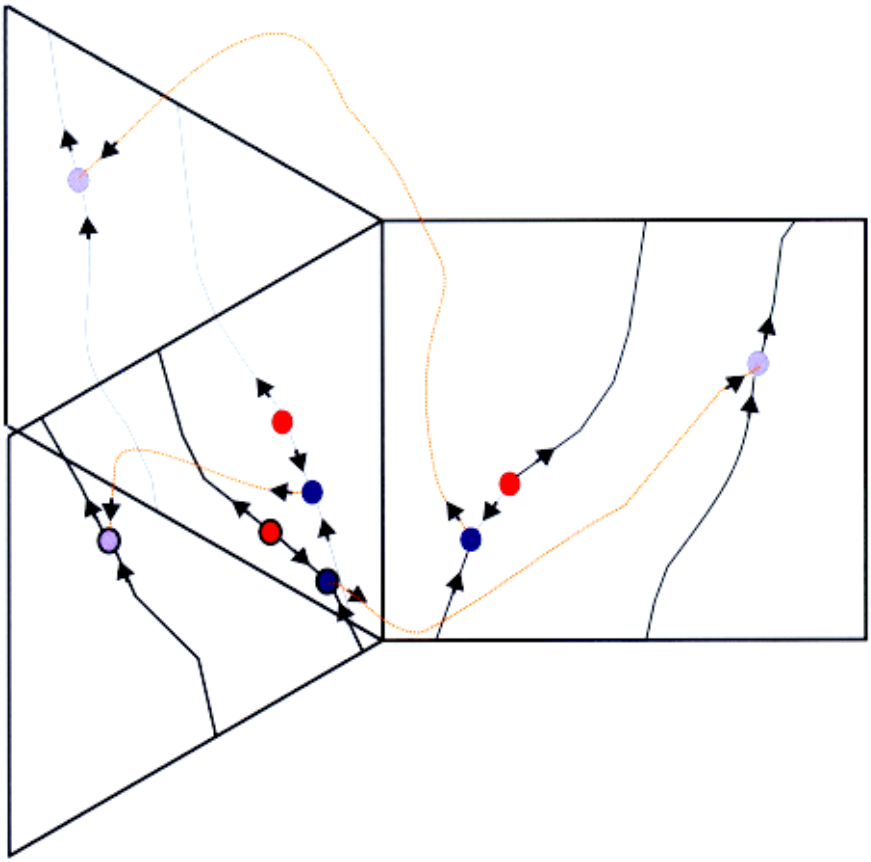

Fig. 10. Heteroclinic connection. Symmetric representation.

We can then prove that there will be a periodic orbit and that the symmetry of this orbit will be of type A, that is, it will be a rotating wave. The demonstration uses only symmetry arguments and unicity of first-order O.D.E.

By hypothesis, there is a solution to our system $\alpha(t)$ satisfying $\alpha(0) = \overline{q}$ and $\alpha(\tau) = \overline{q}'$.

By equivariance of the problem, another solution exists,

$$\alpha'(t) = \gamma \cdot \alpha(t) \tag{28}$$

satisfying

$$\alpha'(0) = \overline{q}' \quad \alpha'(\tau) = \overline{q}'' \,. \tag{29}$$

Since our system is not time dependent, and so it is time translational invariant, we have a solution $\tilde{\alpha}$ satisfying:

$$\tilde{\alpha}(t) = \alpha'(t - \tau) \tag{30}$$

$$\tilde{\alpha}(\tau) = \overline{q}' \quad \tilde{\alpha}(2\tau) = \overline{q}'' \,. \tag{31}$$

Using the unicity of solutions we can conclude that:

$$\alpha(t) = \tilde{\alpha}(t) \tag{32}$$

so $\alpha(2\tau) = \overline{q}''$. In the same way $\alpha(3\tau) = \overline{q}''' = \overline{q}$ (the cycle (312) has order 3), i.e. the solution $\alpha(t)$ is periodical with period $\mathcal{T} = 3\tau$.

From Eqs. (28) and (30) we obtain:

$$\gamma \cdot \alpha(t) = \alpha'(t) = \alpha(t + \tau) = \alpha\left(t + \frac{\mathcal{T}}{3}\right) \tag{33}$$

i.e. $\alpha$ is a periodic solution of Type A. The temporal action of translating time in a third of the period is equivalent to the spatial action of the cycle (312).

A representation of the periodic orbit A and its conjugate in phase space are shown in Fig. 11, and the temporal series of Type A periodical orbit are shown in Fig. 12.

It is also important to remark that the fixed point $P$ is nonhyperbolic. The problem of homoclinic bifurcations with nonhyperbolic fixed points has been studied in [Deng, 1990].

If we keep lowering $\varepsilon$ in the parameter space, we will cross the curve $\alpha$ and find the inverse of the triple transcritic bifurcation, $P1$ gains stability and the periodic orbit disappears. (Notice that our trip

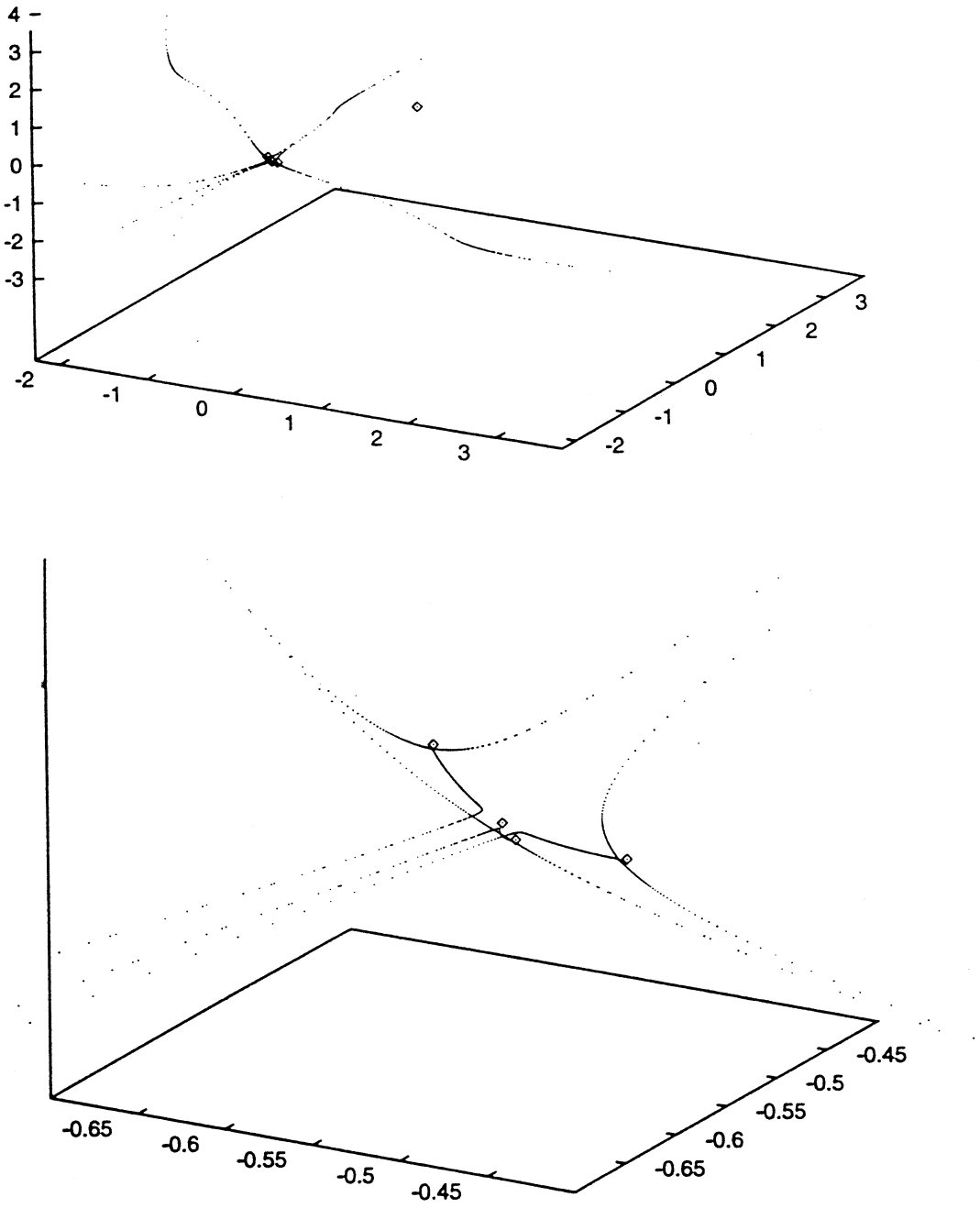


Fig. 11. Solutions in Zone IV. Fixed points $P1$, $P2$, $P3$ and the two periodic solutions Type A. The first graph shows all the phase space, and the second one is in a neighborhood of the fixed points $P3$.

between the three tori ends when we get close to $P3$ because there we are attracted by $P1$.)

Let us come back to Region IV (before crossing the curve $\alpha$) and let us now move, for a fixed $\varepsilon$ in the increasing $\mu$ direction. We then find the curve $\beta$. This curve corresponds to the collapse of $P3$ and $P4$ in a saddle-node bifurcation. This collapse happens in the presence of a global connection between the saddle and the node (Fig. 13). We then expect a periodic orbit from this Andronov bifurcation.

All this analysis has been restricted to one of the invariant tori $\theta i = \theta j$. This periodic orbit will then live in the tori and thus correspond to two in phase oscillator orbit i.e. a Type B orbit, other periodic solutions were expected in Hopf Bifurcations with $D3$ [Golubitsky *et al.*, 1988].

This periodic orbit is the only attractor in each of the invariant tori, but is not globally stable: initial conditions out of the tori still have the rotating wave as limit set.

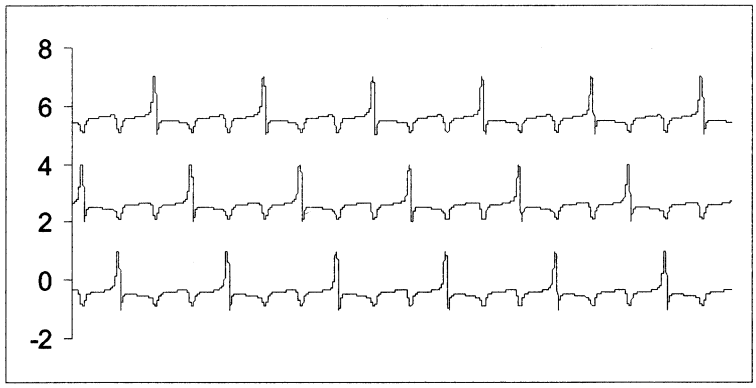


Fig. 12. Temporal series of Type A periodic solution. Series correspond to: (1) $\sin(\theta_1)$, (2) $3+\sin(\theta_2)$, (3) $6+\sin(\theta_3)$.

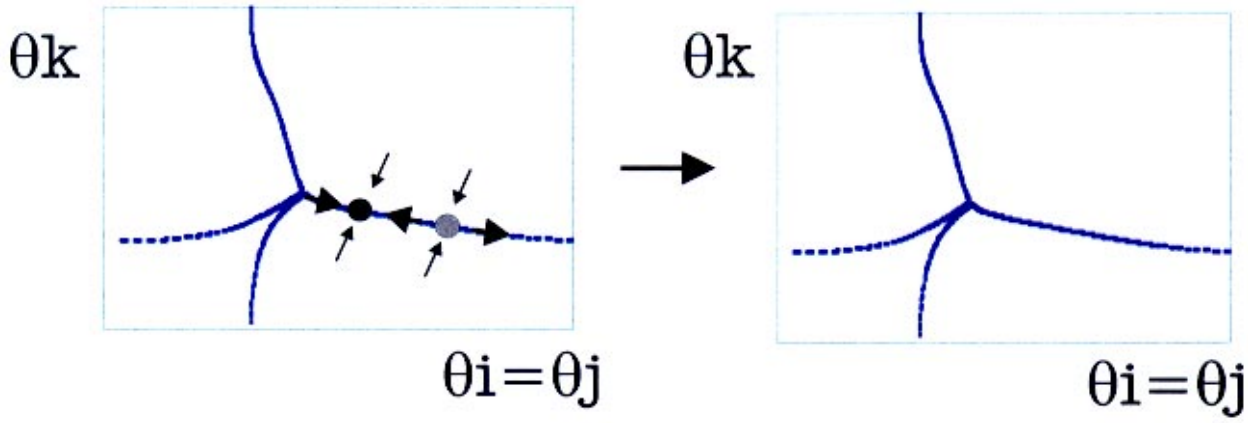


Fig. 13. Type B solution appears when crossing $\beta$ curve in an Andronov bifurcation in one of the invariant two-tori.

How can we measure the stability of B? Figure 14 summarizes the situation, B exists when $P3$ and $P4$ collapse in the saddle-node corresponding to $\beta$ curve and $P5$ and $P6$ collapse in the saddle-node corresponding to $\psi$ curve. $P3$ and $P4$ collapse in a region where the two-tori is locally unstable and $P5$ and $P6$ in a region where it locally attracts. If we are close (in parameter space) to the collapse of $P5$ and $P6$, ($\psi$ curve), the dynamics will be very slow in the region where the orbit locally attracts, and fast where it locally expels, so the orbit will be globally stable. If we are close to the collapse of $P3$ and $P4$ ($\beta$ curve), the dynamics will be slow in the region where the orbit locally expels and fast where it locally attracts and thus it will be globally unstable. We expect a curve in between $\psi$ and $\beta$ where the B solution changes stability. This curve, which we call $\delta$ is numerically calculated by computing the stability of the fixed point associated with this periodic orbit by a Poincaré map. In Fig. 15 temporal series of Type B solution for parameter values close to curves $\psi$ and $\beta$ are shown. Figure 16 shows the coexistence in Region V of the stable A solution with the unstable B solution.

How is the vector field globally reorganized after B changes stability? Our numerical explorations suggest that close to the parameter set for which A disappears, very close to the curve B, there is a region of the parameter space in which a coexistence takes place between those two solutions. This suggests that B emits an unstable solution when it changes stability that eventually collapses with A. Above the $\tau$ curve, in the Region VII, B is stable and A does not exist.

For $\mu$ large enough, Type A solutions can double their period before disappearing in the collapse with the unstable solution emitted by B. This period doubling bifurcation is indicated by curve $\lambda$

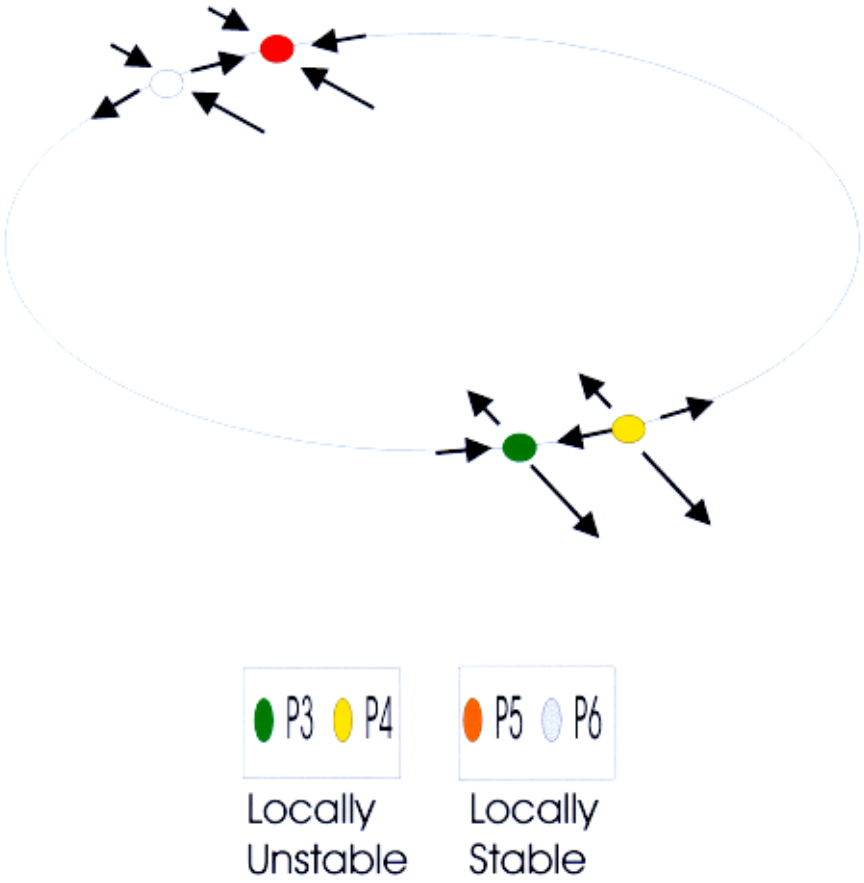


Fig. 14. Type B solution exists when $P3$–$P4$ and $P5$–$P6$ collapse in two saddle-node bifurcations. The first one ($P3$–$P4$) occurs in a region of the invariant two-tori which is locally unstable, the second ($P5$–$P6$) in a region where it is locally stable. Stability of B will result from the competition of these two saddle-nodes.

and the solution with double period is referred to as 2A (Fig. 17). Again there is a small region in parameter space (Region VIII) of coexistence between the solution 2A and the stable Type B periodic orbit. For larger $\mu$ values, this period doubling cascade happens before B changes stability and we find, crossing the $\xi$ curve, (Region X) a strange attractor (Fig. 18), which will again coexist in a short region of parameter space (Region XI) with the stable Type B solution.

### 4.3. *Three coupled oscillators*

If we continue increasing $\mu$, we cross, at $\mu = 1$, the $\kappa$ curve ($\mu = 1$). At this point, each of the uncoupled cells goes through an Andronov bifurcation, and start an oscillatory behavior rather than an excitable one. Since the manifold $\theta_1 = \theta_2 = \theta_3$ is invariant, and restricted to this manifold the three cells are uncoupled, $\mu = 1$ will be a bifurcation point for the three cells system.

We will restrict our analysis to this invariant circle. At $\mu = 1$ the fixed points $P1$ and $P2$ collapse in an Andronov bifurcation, in which a periodic orbit appears, which we call C.

Since we have the analytic expression for this orbit (the circle $\phi = 0$) we can compute analytically the stability of the orbit.

The vector field at any point of the circle will be tangent to it, which we can conclude from its invariance. That is, the vector field will be $\overline{f} = s(\Theta)\hat{\Theta}$.

The differential of the vector field at a point $(\Theta, \phi = 0)$ is:

$$\mathbf{Df}(\Theta, \phi = \mathbf{0}) = \begin{pmatrix} \sin(\Theta) & 0 & 0 \\ 0 & \sin(\Theta) + 3\varepsilon\cos(\Theta) & 0 \\ 0 & 0 & \sin(\Theta) + 3\varepsilon\cos(\Theta) \end{pmatrix}$$

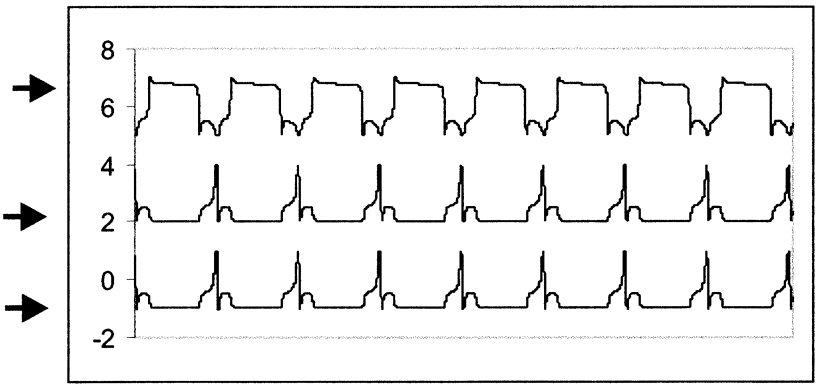


(a)

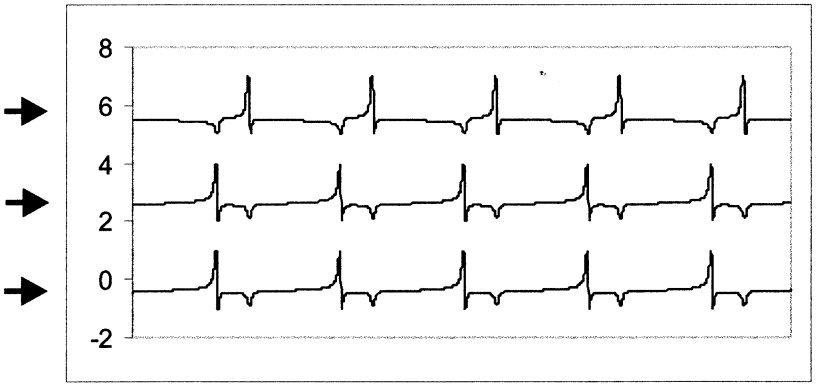


(b)

Fig. 15. Temporal series of Type B periodic solution. (a) Close to the collapse of $P3$ and $P4$ ($\beta$ curve) and (b) Close to the collapse of $P5$ and $P6$ ($\psi$ curve). Series correspond to: (1) $\sin(\theta_1)$, (2) $3+\sin(\theta_2)$ and (3) $6+\sin(\theta_3)$. The arrows represent fixed point (a) $P3$ and (b) $P5$ close to the bifurcation point.

Then, the vector field can be written as:

$$\begin{aligned}\dot{\Theta} &= \mu - \cos(\Theta)\\ \dot{u} &= (\sin(\Theta) + 3\varepsilon\,\cos(\Theta))u + O(\|(u,\,v)\|^2)\\ \dot{v} &= (\sin(\Theta) + 3\varepsilon\,\cos(\Theta))v + O(\|(u,\,v)\|^2)\end{aligned} \tag{34}$$

or:

$$\begin{aligned}\dot{\Theta} &= \mu - \cos(\Theta)\\ \dot{r} &= (\sin(\Theta) + 3\varepsilon\,\cos(\Theta))r + O(r^2)\end{aligned} \tag{35}$$

where $r = \|(u,\,v)\|$. We can write the second equation of [Eqs. (34)] in the following way:

$$\frac{dr}{dt} = g(\Theta)r \Rightarrow \frac{dr}{d\Theta}\dot{\Theta} = g(\Theta)r \tag{36}$$

where $g(\Theta) = \sin(\Theta) + 3\varepsilon\,\cos(\Theta)$, substituting in the first equation of [Eqs. (33)] we obtain:

$$\frac{dr}{r} = \frac{g(\Theta)}{\mu - \cos(\Theta)}d\Theta \tag{37}$$

which we can integrate:

$$\frac{r_f}{r_i} = e^{\int_0^{2\pi}\frac{g(\theta)}{\mu-\cos(\theta)}d\theta} \tag{38}$$

We can see that if after a cycle ($\Theta$ from 0 to $2\pi$) the integral is negative, $r_f < r_i$ the orbit attracts, and if it is positive. $r_f > r_i$ and the orbit expels.

Let us then analyze the sign of the integral:

$$\int_0^{2\pi}\frac{\sin(\theta) + 3\varepsilon\,\cos(\theta)}{\mu - \cos(\theta)}d\theta \tag{39}$$

The first term is an odd function of $\theta$, so it will not contribute to the integral in one cycle. The integral of the second term is positive. This can be shown by just solving it, but we prefer to do it in a way so we can illustrate the concepts remarked when we qualitatively analyzed the stability of B.

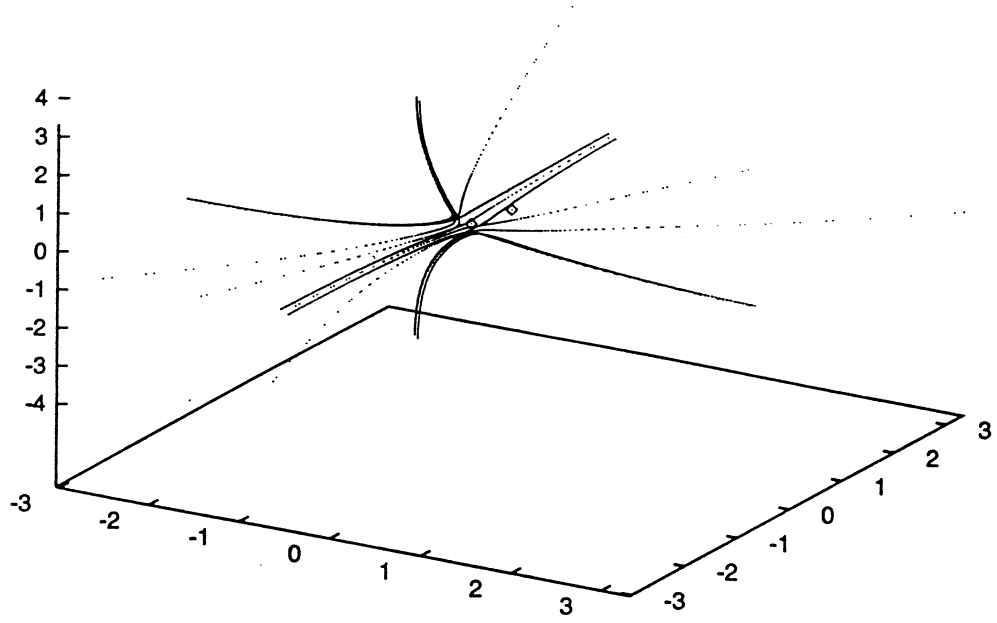


Fig. 16. Region V. Type A is stable, Type B unstable and the fixed points are $P1$ and $P2$.

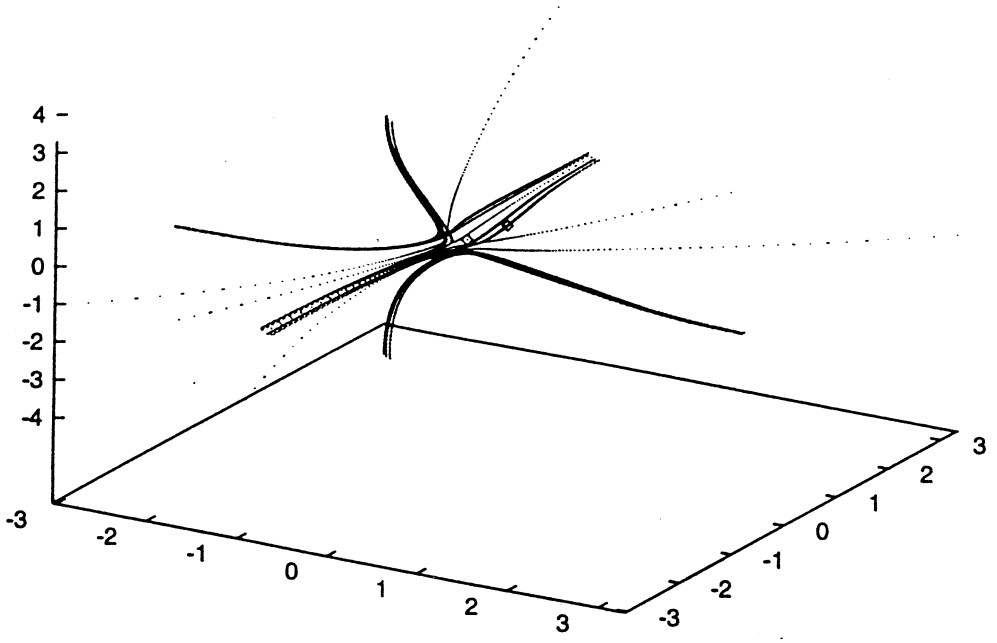


Fig. 17. Region IX. Type B is unstable, 2A is stable and the fixed points are $P1$ and $P2$.

For each $\theta$ with $\cos(\theta) > 0$ (in the first or fourth quadrant),

$$\frac{3\varepsilon \cos(\theta)}{\mu - \cos(\theta)} \tag{40}$$

gives a positive contribution to the integral.

We can write this contribution as the product of two terms: $3\varepsilon \cos(\theta)$ which is a part of the normal component of the vector field, weighted by $1/(\mu - \cos(\theta))$ which is the inverse of the tangential component of the vector field.

For each of those points of the first or fourth quadrant, we have a conjugate by reflection in the $\hat{y}$ axis. At this point the cosine changes sign, so the contribution of the normal component of the vector field is of the same modulus and opposite sign. But for this point, $\cos(\theta) < 0$ and so the weight

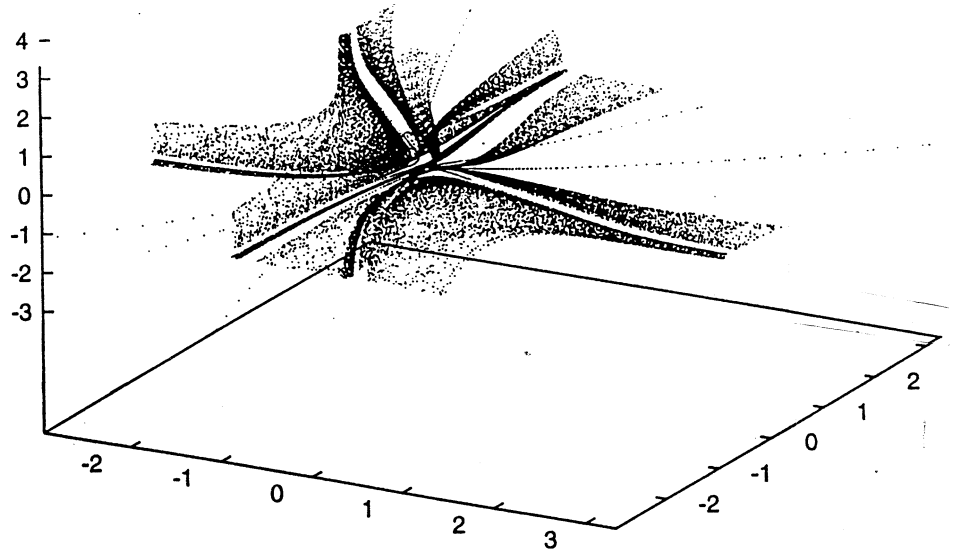


Fig. 18. Zone $X$, strange attractor.

is smaller, because the tangential component of the vector field $\mu - \cos(\theta)$ is bigger than for its conjugate, i.e. we go faster through this point, and then we go faster in the region where the orbit locally attracts than where it locally expels. So, the integral in one cycle is positive, and then, for $\varepsilon > 0$ the orbit C is unstable.

This bifurcation produces no changes in the dynamics outside of the invariant manifold. The solutions outside $\theta_1 = \theta_2 = \theta_3$ are the same in Region X and Region XIV, and in general, when crossing the $\kappa$ curve.

For $\mu > 1$ and below the curve $\psi$, we can prove, assuming no fixed points in the invariant tori, the existence of B orbits.

Let us consider the map from the tori $\theta_i = \theta_j$ to the ring, with its borders identified as we see in Fig. 19. We cut through the circle, $\theta_1 = \theta_2 = \theta_3$,

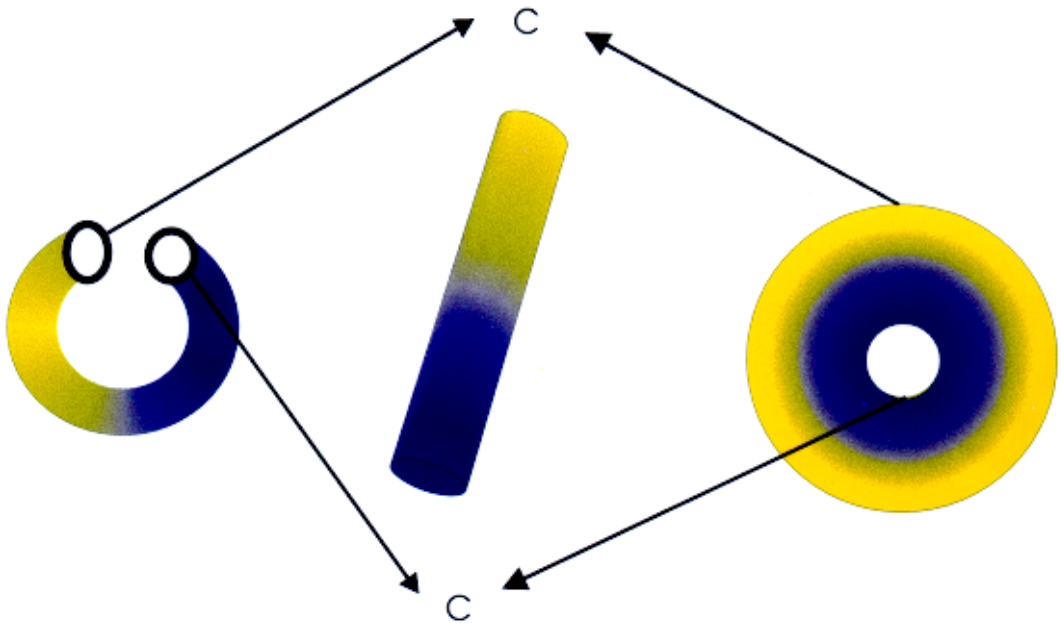


Fig. 19. Map from the tori to a ring with identified borders.

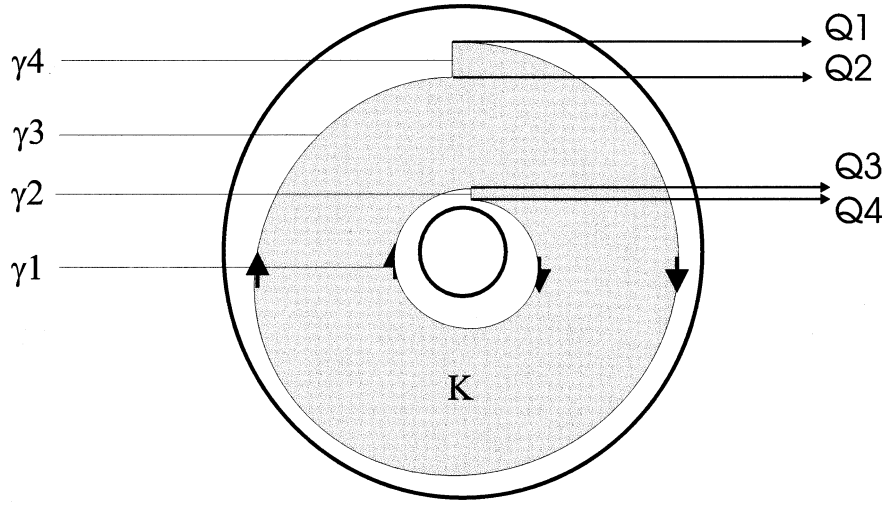


Fig. 20. The invariant compact set corresponds to the region in between curves $\gamma_1 \cdot \gamma_2$ and $\gamma_3 \cdot \gamma_4$.

obtaining a cylinder that we map to the plane in the following way:

$$(z, \theta) \to (r_{\min} + z, \theta) \tag{41}$$

where $\theta$ is the angular variable of the ring. The periodic orbit C corresponds to the trajectory with $r = r_{\min}$ or $r = r_{\max}$ which are, due to the quotient, the same circle (Fig. 19).

The technique consists in finding a compact set K in the interior of the ring, in which the dynamics is invariant. The Poincaré–Bendixon theorem [Hirsch & Smale, 1974] and the nonexistence of fixed points, will guarantee the existence of a periodic orbit.

The mapping was necessary because the Poincaré–Bendixon theorem is valid for compact sets included in $R^2$. The invariant compact set is obtained in the following way (Fig. 20). Consider a point $p_1$ close enough to $r_{\min}$ so that for its orbit, the linear stability analysis of the orbit C is valid. There is then a well defined return map, and due to the instability of C, the image of $p_1$ through this map, will correspond to a point $p_2$, that satisfies $\|p_2\| > \|p_1\|$. We can do the same thing with a point $q_1$ close enough to $r_{\max}$ and with the same arguments, $q_2$ with $\|q_2\| < \|q_1\|$ will be its image after a cycle.

Let $\gamma_1$ be the trajectory from $p_1$ to $p_2$ and let $\gamma_2$ be the segment joining $p_1$ and $p_2$. In the same way, let $\gamma_3$ be the orbit from $q_1$ to $q_2$ and $\gamma_4$ the segment from $q_1$ to $q_2$. The tangential component of the vector field in $r_{\min}(r_{\max})$ is positive (because C is a periodic orbit), that is, $\dot{\theta}(r_{\min}) > 0$, and because the vector field is continuous, we can assume that $p_1(q_1)$ is close enough to $r_{\min}(r_{\max})$ in order for $\dot{\theta}$ to be positive in $\gamma_2(\gamma_4)$, That is, those segments are transversal sections.

From all this it turns out that the region bounded by $\gamma_1 \cdot \gamma_2$ and $\gamma_3 \cdot \gamma_4$ is invariant, because we cannot cross $\gamma_1$ because we would be crossing flux lines, and we cannot cross $\gamma_2$ because $\dot{\theta} > 0$ in the segment. The same analysis is valid for $\gamma_3$ and $\gamma_4$.

We found an invariant compact set in the plane, with no fixed points, so a periodic orbit must exist. This periodic orbit is included in the invariant manifold $\theta_i = \theta_j$ and thus will be a Type B orbit.

## 5. Conclusions

In this work we report an exhaustive study of the collective behavior of three excitable cells coupled in such a way that the system displayed a $D_3$ symmetry. We find periodic solutions in the parameter range where each cell cannot oscillate by itself. There are many studies [Muller *et al.*, 1994] of global behavior of extended systems with local excitable behavior. The periodic orbits reported in this work constitute a low dimensional example of oscillating collective behavior with local excitable dynamics.

All the periodic orbits that we found appeared qualitatively in the same way: after the collapse of two fixed points in a nonhyperbolic fixed point

with a heteroclinic or homoclinic connection between them. For this reason, the orbits are born with infinite period and nonzero amplitude. The connections were in most cases possible due to the existence of invariant subspaces that allows us to explain the origin of the symmetries of the periodic solutions. We found that the symmetry of the periodic bifurcation appearing in global bifurcations involving the breaking of heteroclinic connections are the same as those expected in Hopf (local) bifurcations.

## Acknowledgments

We thank Dr. J. D. Rossi for discussions, encouragement and support and Tim Gardner for reading and his comments on the manuscript.

## References

Andronov, A. A., Leontovich, E. A., Gordon, J. I. & Majer, A. J. [1973] *Theory of Bifurcations of Dynamical Systems are a Plane* (Wiley, NY).

Ashwin, P., King, G. P. & Swift, J. W. [1990] "Three identical coupled oscillators with symmetry," *Nonlinearity* **4**, 585–603.

Deng, B. [1990] "Homoclinic bifurcations with nonhyperbolic equilibria," *SIAM J. Math. Anal.* **21**(3), 693–720.

Giudicci, M., Green, C., Giacomelli, G., Nespolo, U. & Tredicce, J. R. [1997] "Andronov bifurcation and excitability in semiconductor lasers with optical feedback," *Phys. Rev.* **E55**(6), 6414–6418.

Golubitsky, M., Stewart, M. & Schaeffer, I. [1988] *Singularities and Groups in Bifurcation Theory*, Vol. II (Springer-Verlag).

Hirsch, M. W. & Smale, S. [1974] *Differential Equations Dynamical Systems and Linera Albebra* (Academic Press, NY).

Hodgin, A. L. & Huxley, A. F. [1954] "A quantitative description of membrane current and its application to conduction and excitation in nerve," *J. Physiol.* **117**, 500–544.

Muller, S. C., Coullet, P. & Walgraef, D. [1994] "From oscillations to excitability: A case study in spatially extended systems," *Chaos* **4**(3), 439–442.

Murray, J. D. [1989] *Mathematical Biology* (Springer-Verlag).

Solari, H. G., Natiello, M. A. & Mindlin, G. B. [1996] *Nonlinear Dynamics. A Two-Way Trip from Physics to Math.* (IOP Publishers, London).

Wiggins, S. [1990] *Introduction to Applied Nonlinear Dynamical Systems and Chaos* (Springer-Verlag).

Zimmerman, M. G. & Natiello, M. A. [1998] "Homoclinic and heteroclinic bifurcations close to a twisted heteroclinic cycle," *Int. J. Bifurcation and Chaos* **8**(2), 359–375.